C−O and C−S Bond Cleavage in Chelating Diethers and Thioethers Promoted by η^9,η^5-Bis(indenyl)zirconium Sandwich Complexes: A Combined Experimental and Computational Study

Christopher A. Bradley,† Luis F. Veiros,‡ and Paul J. Chirik*,†

Department of Chemistry and Chemical Biology, Baker Laboratory, Cornell University, Ithaca, New York 14853, and Centro de Quimica Estrutural, Complexo I, Instituto Superior Técnico, Avenida Rovisco Pais 1, 1049-001 Lisbon, Portugal

Received February 5, 2007

Gently warming the η^6,η^5-bis(indenyl)zirconium dimethoxyethane compound (η^6-C_9H_5-1,3-$(SiMe_3)_2$)-(η^5-C_9H_5-1,3-$(SiMe_3)_2$)Zr(DME) (**1-DME**) to 45 °C resulted in C−O bond scission to yield an equimolar mixture of the zirconocene ethylene compound (η^5-C_9H_5-1,3-$(SiMe_3)_2)_2$Zr(η^2-CH_2═CH_2) and the corresponding zirconium bis(methoxide) complex (η^5-C_9H_5-1,3-$(SiMe_3)_2)_2$Zr$(OMe)_2$. Monitoring the relative rates of **1-DME** versus **1-DME-*d*$_{10}$** cleavage by ^{1}H NMR spectroscopy established no kinetic isotope effect (k_H/k_D = 1.0(1)), eliminating the possibility of C−H activation in or prior to the rate-determining step. Computational studies support a pathway involving rate-determining DME dissociation from the η^6,η^5-bis(indenyl)zirconium complex followed by facile η^6 to η^5 indenyl haptotropic rearrangement and C−O bond scission. Corresponding C−S bond cleavage chemistry has been investigated for three thioethers and the mechanism of bond activation compared to the oxygen congeners.

Introduction

The synthesis, isolation,[1] and structural[2] characterization of η^9,η^5-bis(indenyl)zirconium sandwich complexes, (η^9-C_9H_5-1,3-R_2)(η^5-C_9H_5-1,3-R_2)Zr (R = silyl, ^{i}Pr), has allowed the study of fundamental coordination chemistry at a reduced zirconium center. While one of the indenyl rings adopts unusual η^9 hapticity in the ground state,[2,3] NMR spectroscopic studies have demonstrated rapid interconversion of η^9 and η^5 coordination modes at ambient temperature in solution. Computational studies support a pathway whereby the linear, $S = 0$ sandwich complex (η^5-C_9H_5-1,3-$R_2)_2$Zr is accessed by dissociation of the benzo fragment of the η^9 ring (eq 1).[4]

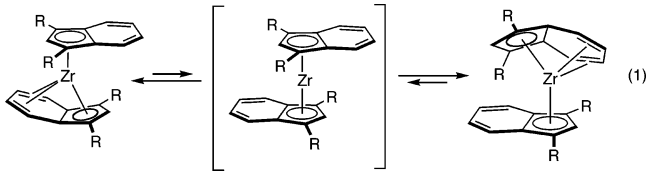

(1)

The intermediate [(η^5-C_9H_5-1,3-$R_2)_2$Zr] species has proven to be a powerful two-electron reductant. The bis(indenyl)-zirconium sandwich complexes (η^9-C_9H_5-1,3-R_2)(η^5-C_9H_5-1,3-R_2)Zr (R = $SiMe_3$, **1**; = $SiMe_2Ph$, ^{i}Pr, **5**) react rapidly with olefins to form metallocyclopentanes or C−H activated products depending on the alkene and indenyl substituents.[2] Coupling chemistry is also observed with alkynes,[1,2] rendering the η^9,η^5-bis(indenyl)zirconium compounds isolable forms of the well-known, in-situ-generated Negishi reagent, [(η^5-$C_5H_5)_2$Zr],[5] which has been shown to be a complex mixture of Zr(III) and Zr(IV) compounds.[6] In more recent chemistry, both **1** and **5** were found to promote C−O bond cleavage in simple aliphatic ethers: MeOR (R = Et, ^{n}Bu, ^{t}Bu), Et_2O, and $^iPr_2O$ (Figure 1).[7] For acyclic ethers, kinetic isotope effects, rate studies, preparation of model compounds and product distributions support a mechanism involving rate-determining C−H activation to yield an η^5,η^5-bis(indenyl)zirconium alkyl hydride intermediate, which undergoes rapid β-alkoxide elimination to yield the observed products.

Sufficiently nucleophilic ethers such as THF are known to induce η^9 to η^6 haptotropic rearrangement to yield isolable η^6,η^5-bis(indenyl)zirconium−THF compounds.[8] Warming benzene-d_6 solutions of **1-THF** (R = $SiMe_3$) to 85 °C also resulted in C−O bond cleavage to yield the corresponding alkyl−alkoxy zirconocycle (Figure 1).[7] Both experimental and computational studies support a pathway involving initial THF dissociation, followed by η^6 to η^5 indenyl haptotropic rearrangement to yield the [(η^5-C_9H_5-1,3-$R_2)_2$Zr] species, which then promotes rate-determining C−H activation followed by C−O bond scission. In this contribution, we further explore C−O and C−S bond cleavage with bis(indenyl)zirconium sandwich complexes and report that the preferred pathway for bond scission is substrate dependent.

Results and Discussion

C−O Bond Cleavage in Dialkyl Diethers. As described previously,[8] treatment of the silylated bis(indenyl)zirconium

* Corresponding author. E-mail: pc92@cornell.edu.
† Cornell University.
‡ Instituto Superior Técnico.

(1) Bradley, C. A.; Lobkovsky, E.; Chirik, P. J. *J. Am. Chem. Soc.* **2003**, *125*, 8110.
(2) Bradley, C. A.; Keresztes, I.; Lobkovsky, E.; Young, V. G.; Chirik, P. J. *J. Am. Chem. Soc.* **2004**, *126*, 16937.
(3) Veiros, L. F. *Chem.−Eur. J.* **2005**, *11*, 2505.
(4) Veiros, L. F. *Organometallics* **2006**, *25*, 2266.
(5) (a) Negishi, E.-I.; Takahashi, T. *Acc. Chem. Res.* **1994**, *27*, 124. (b) Rosenthal, U.; Pellny, P.-M.; Kirchbauer, F. G.; Burlakov, V. V. *Acc. Chem. Res.* **1994**, *27*, 14.
(6) Dioumaev, V. K.; Harrod, J. F. *Organometallics* **1997**, *16*, 1452.
(7) Bradley, C. A.; Veiros, L. F.; Pun, D.; Lobkovsky, E.; Keresztes, I.; Chirik, P. J. *J. Am. Chem. Soc.* **2006**, *128*, 16600.
(8) Bradley, C. A.; Lobkovsky, E.; Keresztes, I.; Chirik, P. J. *J. Am. Chem. Soc.* **2005**, *127*, 10291.

10.1021/om0701120 CCC: $37.00
Publication on Web 05/22/2007

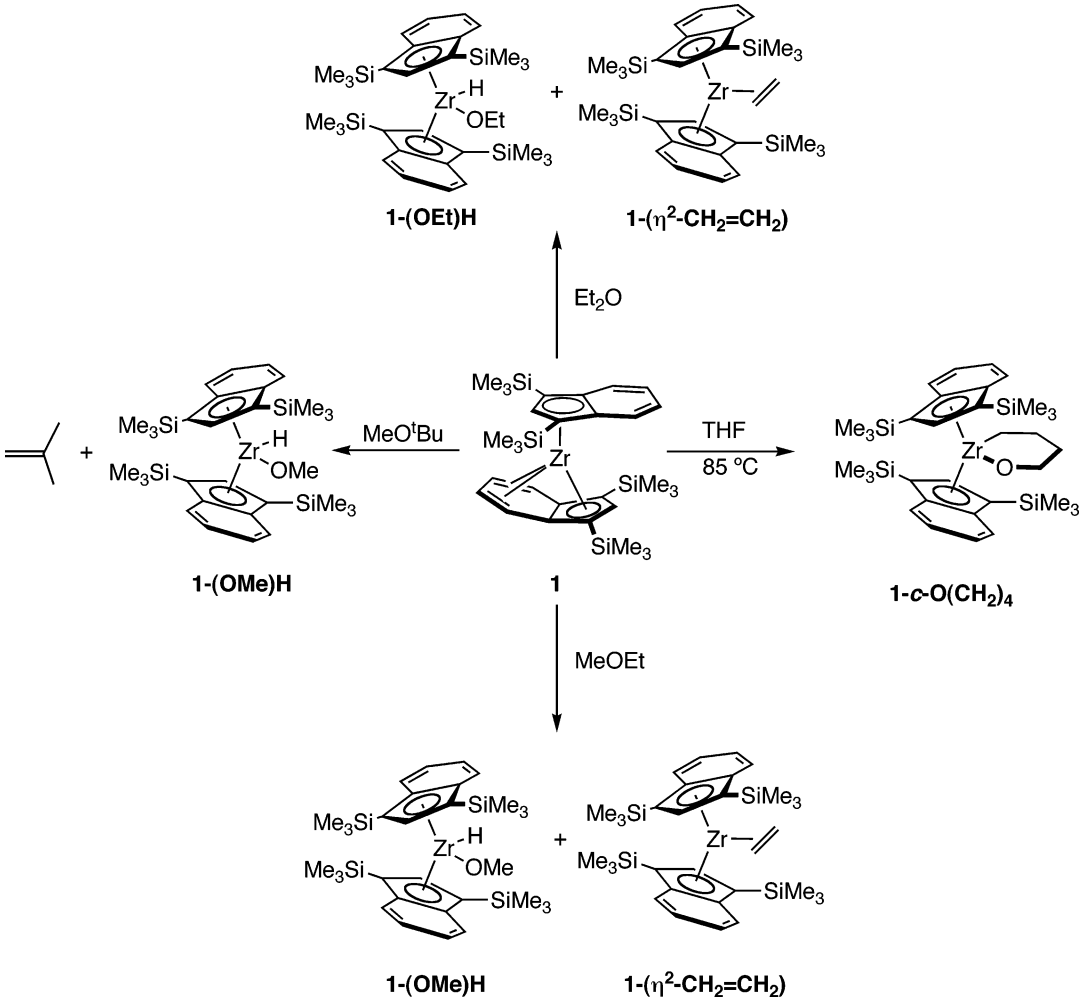

Figure 1. Carbon−oxygen bond cleavage in dialkyl ethers and THF promoted by η^9,η^5-bis(indenyl)zirconium sandwich complexes.

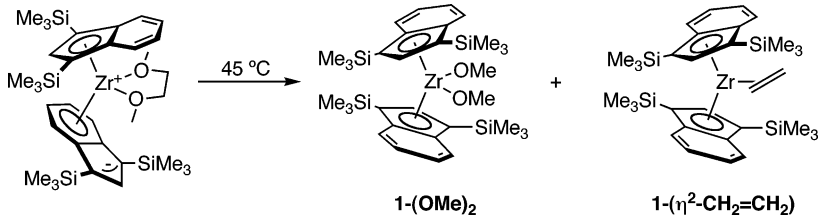

Figure 2. DME cleavage promoted by η^9,η^5-bis(indenyl)zirconium sandwich complex **1**.

sandwich complex, **1**, with DME furnished (η^6-C_9H_5-1,3-$(SiMe_3)_2$)(η^5-C_9H_5-1,3-$(SiMe_3)_2$)Zr($MeOCH_2CH_2OMe$) (**1-DME**), as a green crystalline solid. Both X-ray diffraction and NMR spectroscopic studies confirmed the η^6,η^5 hapticity of the indenyl rings. Mild thermolysis of a benzene-d_6 solution containing **1-DME** at 45 °C yielded a near equimolar mixture of the bis(indenyl)zirconium ethylene compound **1-(η^2-CH_2=CH_2)** and the zirconocene bis(methoxide) (η^5-C_9H_5-1,3-$(SiMe_3)_2)_2$Zr-$(OCH_3)_2$ (**1-$(OMe)_2$**) (Figure 2). No attempt was made to separate the two products.

The origin of the ethylene compound **1-(η^2-CH_2=CH_2)** was probed by treatment of **1-DME** with free CH_2=CH_2. Immediately upon careful addition of 1 equiv of the olefin, displacement of the ether was observed, quantitatively forming **1-(η^2-CH_2=CH_2)**. As with diethyl ether cleavage,[7] the displacement of DME from **1-DME** during the course of the reaction accounts for the observed olefin complex.

The scope of chelating diethyl cleavage was explored with two additional substrates, 1,2-diethoxyethane (DEE) and 2,3-dimethoxybutane (DMB). Both of these molecules are known to induce haptotropic rearrangement in **1** to yield the corresponding η^6,η^5-bis(indenyl)zirconium diether complex.[8] Warming a benzene-d_6 solution of **1** to 45 °C in the presence of 10 equiv of DEE yielded **1-(η^2-CH_2=CH_2)** and the zirconocene alkoxy hydride complex (η^5-C_9H_5-1,3-$(SiMe_3)_2)_2$Zr(OCH_2CH_2-OEt)H (**1-$(O(CH_2)_2OEt)H$**) in near equimolar quantities (Figure 3). Performing a similar thermolysis experiment with **1** and excess DMB at 45 °C yielded **1-(OMe)H** and a mixture of methoxy-substituted olefins. Each of the zirconocene products was characterized by NMR spectroscopy by comparison to authentic samples, with the exception of **1-$(O(CH_2)_2OEt)H$**, which is new to this study. The mixture of methoxy-substituted olefins was characterized by a combination of NMR spectroscopy and mass spectrometry.

Mechanistic Studies of C−O Bond Cleavage in Diethers. Several experiments were conducted to probe the mechanism of C−O bond cleavage in DME, DEE, and DMB. Specifically, it was of interest to compare the preferred pathway for DME

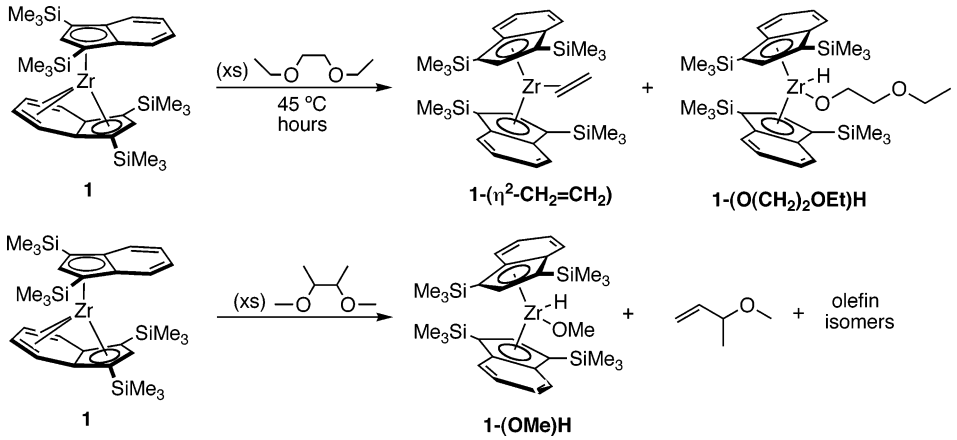

Figure 3. 1,2-Diethoxyethane and 2,3-dimethoxybutane cleavage promoted by **1**.

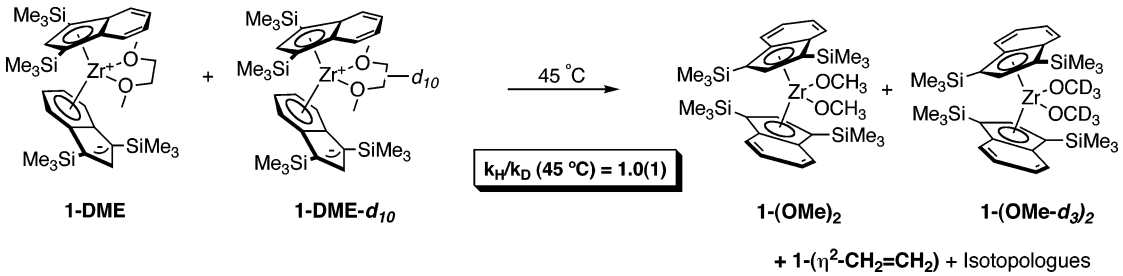

Figure 4. Determination of the kinetic isotope effect for DME cleavage.

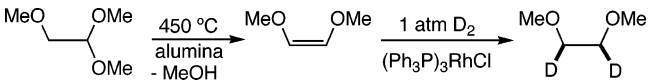

Figure 5. Preparation of *cis*-1,2-d_2-DME.

cleavage to that previously reported for THF, as both substrates yield isolable η^6,η^5-bis(indenyl)zirconium ether compounds. The role of C−H activation in C−O scission was probed by measuring the kinetic isotope effect for the reaction. Heating an equimolar mixture of **1-DME** and **1-DME-*d*$_{10}$** to 45 °C produced the expected isotopologues of the zirconocene ethylene compound and the corresponding bis(methoxide) derivative (Figure 4). The rate of conversion was determined by ^{1}H NMR spectroscopy by integration of the indenyl resonances of both compounds versus the methoxide peaks of **1-(OMe)$_2$**. The ethylene compounds could not be used due to competing cyclometalation pathways that produced isotopic exchange.[7] Using this procedure, a kinetic isotope effect (k_H/k_D) of 1.0(1) was obtained at 45 °C, contrasting the normal primary values observed for diethyl ether and THF cleavage with **1**.

The lack of a normal, primary isotope effect for DME cleavage suggested that C−H activation does not occur in or prior to the rate-determining step for C−O activation as was observed for THF and diethyl ether. Because these results indicated a possible change in mechanism, additional deuterium labeling studies were conducted. One alternative possibility considered was a concerted process whereby ethylene is directly extruded from **1-DME** (or an η^5,η^5-haptomer), yielding **1-(OMe)$_2$**. To experimentally probe if such a process was operative, cleavage of a stereochemically pure **1-DME** isotopologue was targeted.

Preparation of *cis*-1,2-d_2-DME was accomplished as outlined in Figure 5. This substrate was chosen due to its relative ease of synthesis and the ability to differentiate the stereochemistry of *cis*- and *trans*-1,2-d_2-ethylene by gas-phase infrared spectroscopy.[9] Pyrolysis of commercially available dimethoxyacetaldehyde at 450 °C over an alumina column yielded *cis*-1,2-dimethoxyethylene.[10] Deuteration with Wilkinson's catalyst, $(Ph_3P)_3RhCl$, in the presence of 1 atm of D_2 gas furnished the desired product in >95% isotopic purity as judged by ^{1}H NMR spectroscopy.

Addition of *cis*-1,2-d_2-DME to a benzene-d_6 solution of **1** furnished a near equimolar mixture of *syn* and *anti* **1-*cis*-d_2-DME** products. The *syn* and *anti* designators refer to the orientation of the deuterium atoms with respect to the η^6-indenyl ring (Figure 6). Thermolysis of the mixture of isomers at 45 °C followed by degradation of the organometallic products with $PbCl_2$ yielded **1-Cl$_2$** and free ethylene (Figure 6). The volatile olefin was collected and analyzed by gas-phase infrared spectroscopy. The major ethylene isotopologue collected was CH_2═CH_2, not *cis*- or *trans*-1,2-d_2-ethylene (see Supporting Information).

As reported previously,[7] control experiments with the deuterium-labeled ethylene complex **1-(η^2-CD$_2$═CD$_2$)** show that it undergoes isotopic exchange with the [$SiMe_3$] substituents on the indenyl ring via competitive cyclometalation and olefin insertion reactions. Analysis of **1-Cl$_2$** following cleavage of *cis*-1,2-d_2-DME established deuterium incorporation into the [$SiMe_3$] groups, demonstrating that the rate of cyclometalation is competitive with C−O bond cleavage. Because of the competing isotopic scrambling process, any concerted process for DME cleavage cannot be ruled out experimentally.

While open questions remain about the preferred pathway for DME cleavage, the observed products from C−O bond scission in DEE and DMB do provide some insight into the mechanism of cleavage for these substrates. For DEE, observation of **1-(O(CH$_2$)$_2$OEt)H** is consistent with a C−H activation−β-alkoxide elimination event. Initial dissociation of DEE

(9) Dervan, P. B.; Santilli, D. S. *J. Am. Chem. Soc.* **1980**, *102*, 3863.
(10) McElvain, S. M.; Stammer, C. H. *J. Am. Chem. Soc.* **1951**, *73*, 915.

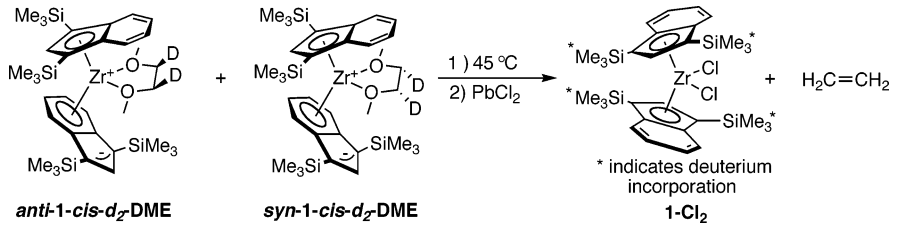

Figure 6. C−O bond cleavage of *cis*-1,2-d_2-DME with **1**.

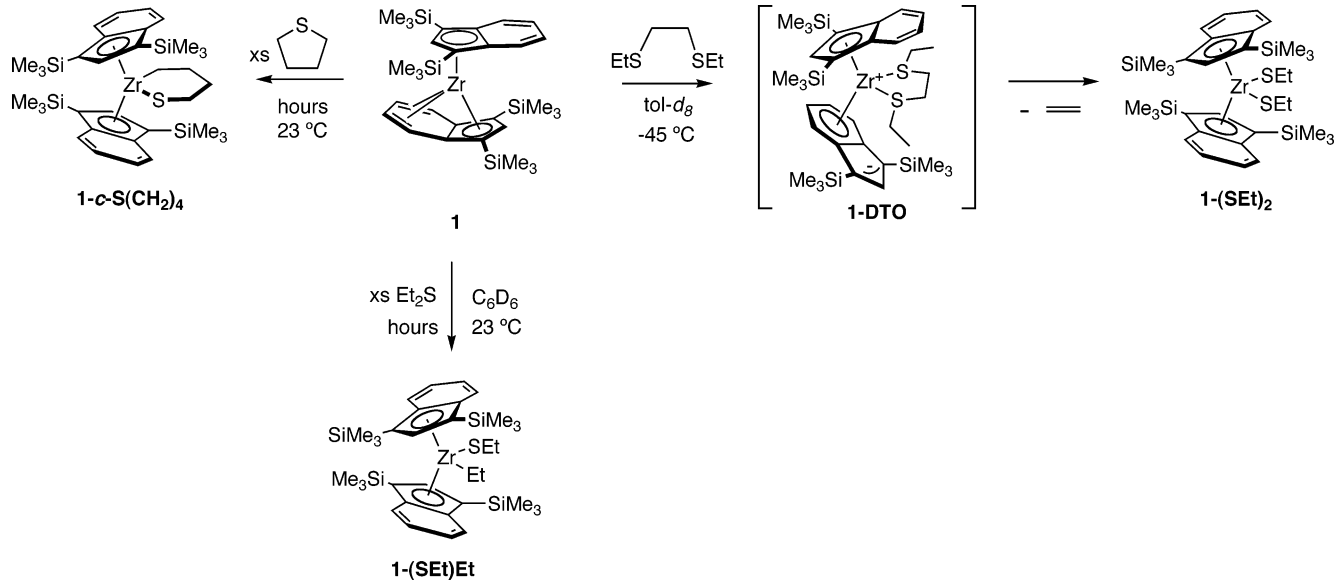

Figure 7. C−S bond cleavage of thioethers with **1**.

from **1-DEE** followed by indenyl haptotropic shift yields [(η^5-C_9H_5-1,3-($SiMe_3$)$_2$)$_2$Zr], which is sufficiently reducing to promote the oxidative addition of a C−H bond of a terminal methyl group in free DEE. Subsequent β-alkoxide elimination liberates ethylene, which is trapped by free **1** or displaces ether from **1-DEE**. This pathway is similar to that proposed for diethyl ether cleavage.[7] A similar sequence of reactions also accounts for the observed products from DMB C−O bond cleavage. In this case, C−H activation of a backbone methyl group followed by β-alkoxide elimination and isomerization of the free olefins accounts for the observed products.

Carbon−Sulfur Bond Cleavage of Thioethers. The possibility of C−S bond cleavage with η^9,η^5-bis(indenyl)zirconium sandwich compounds was also explored with the goal of comparing the results to the oxygenated congeners. This chemistry is also motivated, in part, by the interest to develop new reagents for hydrodesulfurization chemistry.[11−13] Three representative thioethers were examined to compare with their oxygenated congeners: diethyl sulfide, tetrahydrothiophene, and 3,6-dithiaoctane.

Addition of 10 equiv of diethyl sulfide to a benzene-d_6 solution of **1** at 23 °C resulted in cleavage of the C−S bond over the course of hours to yield (η^5-C_9H_5-1,3-($SiMe_3$)$_2$)$_2$Zr(SEt)Et (**1-(SEt)Et**) (Figure 7). Attempts to observe any intermediates along the reaction pathway were unsuccessful. This product contrasts the chemistry observed with diethyl ether, where C−H activation precedes C−O bond scission,[7] and as a result, **1-(η^2-CH_2=CH_2)** and **1-(OEt)H** are observed (Figure 1).

Attempts to observe the η^6,η^5-bis(indenyl)zirconium THT compound in analogy with **1-THF** have been unsuccessful. Addition of excess THT to a benzene-d_6 solution of **1** resulted in C−S bond cleavage to yield the ring-opened alkyl thiolato zirconocene (η^5-C_9H_5-1,3-($SiMe_3$)$_2$)$_2$Zr-(*cyclo*-$S(CH_2)_4$) (**1-*c*-S(CH$_2$)$_4$**) (Figure 7). Although the C−S cleavage product is analogous to the THF ring-opened product, it is noteworthy that **1-*c*-S(CH$_2$)$_4$** forms at 23 °C, while **1-*c*-O(CH$_2$)$_4$** requires heating to 85 °C.[7]

Treatment of a toluene-d_8 solution of **1** with the commercially available chelating bis(thioether), 3,6-dithiaoctane, at −45 °C allowed observation of the η^6,η^5-bis(indenyl)zirconium thioether complex (η^6-C_9H_5-1,3-($SiMe_3$)$_2$)(η^5-C_9H_5-1,3-($SiMe_3$)$_2$)Zr(DTO) (**1-DTO**), demonstrating that certain sulfur donors are sufficiently nucleophilic to induce haptotropic rearrangement. Diagnostic upfield ^{1}H NMR resonances were observed at 4.29 and 4.65 ppm for the benzo and cyclopentadienyl hydrogen, respectively, and are indicative of η^6 indenyl coordination. Warming the toluene-d_8 solution of **1-DTO** to 23 °C resulted in facile C−S bond cleavage to yield the zirconocene bis(thiolate) complex (η^5-C_9H_5-1,3-($SiMe_3$)$_2$)$_2$Zr(SEt)$_2$ (**1-(SEt)$_2$**), along with free ethylene (Figure 7). Observation of free ethylene rather than **1-(η^2-CH$_2$=CH$_2$)** is likely a consequence of the rapid rate of C−S bond cleavage that precludes efficient trapping of the olefin by **1-DTO**.

Observation of **1-(SEt)Et** from diethyl sulfide cleavage is consistent with a mechanistic pathway involving direct C−S activation by the η^9,η^5-bis(indenyl)zirconium sandwich **1** rather than C−H activation. Invoking a similar direct C−S bond

(11) For recent examples of C−H and C−X (X = chalcogen) activation by a molybdenum complex: Churchill, D. G.; Bridgewater, B. M.; Zhu, G.; Pang, K. L.; Parkin, G. *Polyhedron* **2006**, *25*, 499.

(12) Stirling, D. *The Sulfur Problem: Cleaning up Industrial Feedstocks*; RSC Clean Technology Monographs, 2000.

(13) (a) Janak, K. E.; Tanski, J. M.; Churchill, D. G.; Parkin, G. *J. Am. Chem. Soc.* **2002**, *124*, 4182. (b) Angelici, R. J. *Organometallics* **2001**, *20*, 1259.

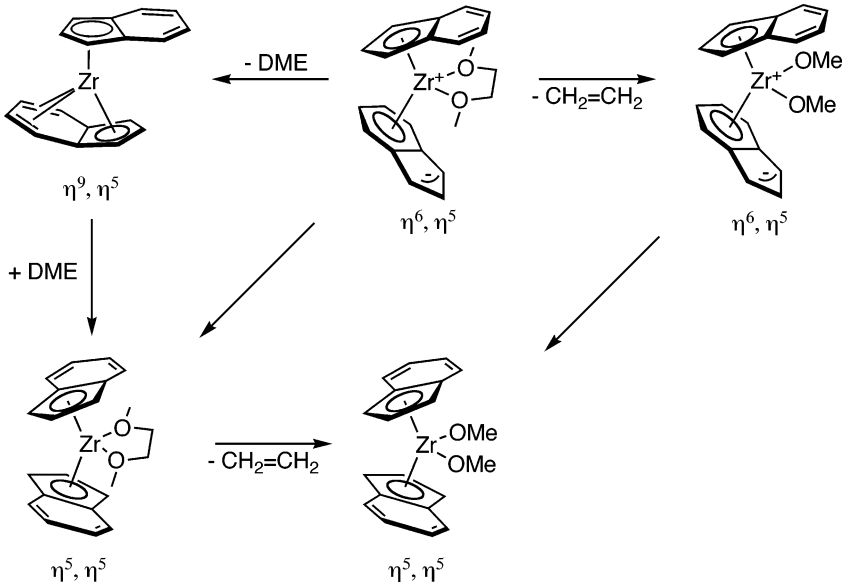

Figure 8. Possible pathways considered computationally for DME cleavage.

activation process for addition of THT and DTO to **1** would also account for the observed products. However, for these substrates, C−H bond activation processes that precede C−S addition cannot be ruled out. Unfortunately, the inaccessibility of deuterated thioethers has prohibited measurement of kinetic isotope effects.

Computational Studies. The observation of a kinetic isotope effect of 1.0(1) for DME cleavage by **1** contrasts the normal, primary KIE values observed for C−O activation with diethyl ether and THF and suggests that C−H bond cleavage reactions were not in or prior to the rate-determining step. One possibility is that DME dissociation from **1-DME** is rate limiting and is followed by fast C−H activation and β-alkoxide elimination events, similar to those proposed for dialkyl ether scission.[7] However, previously reported model studies have demonstrated the kinetic incompetency of the intermediate zirconocene alkoxy hydride species.[7] Because obtaining additional mechanistic data was complicated by competing cyclometalation processes, the preferred pathway for C−O bond cleavage in **1-DME** was investigated by DFT calculations[14] with (η^6-C_9H_7)-(η^5-C_9H_7)Zr($MeOCH_2CH_2OMe$) (**A**), where the sterically demanding [$SiMe_3$] ring substituents were replaced with hydrogens for computational expediency. Previous work has shown that model complexes of this type provide accurate, semiquantitative descriptions of the reaction mechanisms of these compounds.[4,7]

The reaction studied corresponds to the conversion of the initial η^6,η^5-bis(indenyl)zirconium DME complex into the corresponding bis(methoxide) complex, (η^5-C_9H_7)$_2$Zr(OMe)$_2$. There are two major structural changes involved in this transformation. One is C−O bond breaking and the other is the change in hapticity of the indenyl ring from η^6 to η^5 coordination. The different possible pathways for the reaction are summarized in Figure 8.

In one pathway, the reaction may occur directly from the η^6,η^5 complex to initially yield the zirconocene bis(methoxide) complex (η^6-C_9H_7)(η^5-C_9H_7)Zr(OCH_3)$_2$, while maintaining the η^6,η^5 ring hapticity. This complex would then undergo a haptropic shift to yield the final product (right side, Figure 8). Alternatively, the order of the two processes may be reversed, with C−O bond activation occurring after η^6 to η^5 haptotropic rearrangement (left side, Figure 8). The first step in this pathway is the formation of the η^5,η^5-bis(indenyl)zirconium−DME intermediate, (η^5-C_9H_7)$_2$Zr($MeOCH_2CH_2OMe$). This can be achieved either through an intramolecular process corresponding to η^6,η^5 haptotropic rearrangement maintaining DME coordination or by an alternative pathway involving initial DME dissociation to form the η^9,η^5-bis(indenyl)zirconium sandwich complex (η^9-C_9H_7)(η^5-C_9H_7)Zr. Both possibilities are depicted.

All of the mechanisms depicted in Figure 8 were investigated in order to find the most favorable path for the reaction. The free energy profile corresponding to the first one, namely C−O bond activation followed by haptotropic rearrangement, is presented in Figure 9.

The profile depicted in Figure 9 corresponds to a two-step path. In the first step, cleavage of the C−O bonds in **A** yields free ethylene and the η^6,η^5-zirconocene bis(methoxide) complex (η^6-C_9H_7)(η^5-C_9H_7)Zr(OCH_3)$_2$ (**B**), retaining the hapticity of the indenyl ligands. The calculated transition state for C−O bond breaking (**TS$_{AB}$**) is an early one with rather short contacts (d_{C-O} = 1.61 and 1.85 Å), not much longer than the corresponding bond distances in the reagent **A** (d_{C-O} = 1.43 and 1.44 Å) and in the solid-state structure of **1-DME** (d_{C-O} = 1.43 and 1.45 Å). This conclusion is also supported by the C−O Wiberg indices (WI)[15] in **TS$_{AB}$** (WI = 0.446 and 0.642), showing that the transition state is reached with only incipient C−O bond breaking. The formation of the ethylene C=C bond in **TS$_{AB}$** is also just starting ($d_{C=C}$ = 1.45 Å, WI = 1.017) but still far from the values of free ethylene ($d_{C=C}$ = 1.33 Å, WI = 2.039). In the second step, a haptotropic shift between the η^6 and η^5 rings yields the final product, (η^5-C_9H_7)$_2$Zr(OCH_3)$_2$ (**C**). In the corresponding transition state, **TS$_{BC}$**, the shifting indenyl ring has a coordination mode best described as being in between η^6 and η^5 with Zr−C bond breaking of the benzo portion well advanced and, at the same time, the new Zr−C bonds to the C_5 ring are still far from accomplished (see Figure 10 for indenyl labeling). In fact, once **TS$_{BC}$** is reached, the Zr−C_a distance is still long (4.00 Å), corresponding to a very weak interaction (WI = 0.021), while the Zr−$C_{e/e'}$ bonds are already significantly

(14) Parr, R. G.; Yang, W. *Density Functional Theory of Atoms and Molecules*; Oxford University Press: New York, 1989.

(15) (a) Wiberg, K. B. *Tetrahedron* **1968**, *24*, 1083. (b) Wiberg indices are electronic parameters related with the electron density in between atoms. They can be obtained from a natural population analysis and provide an indication of the bond strength.

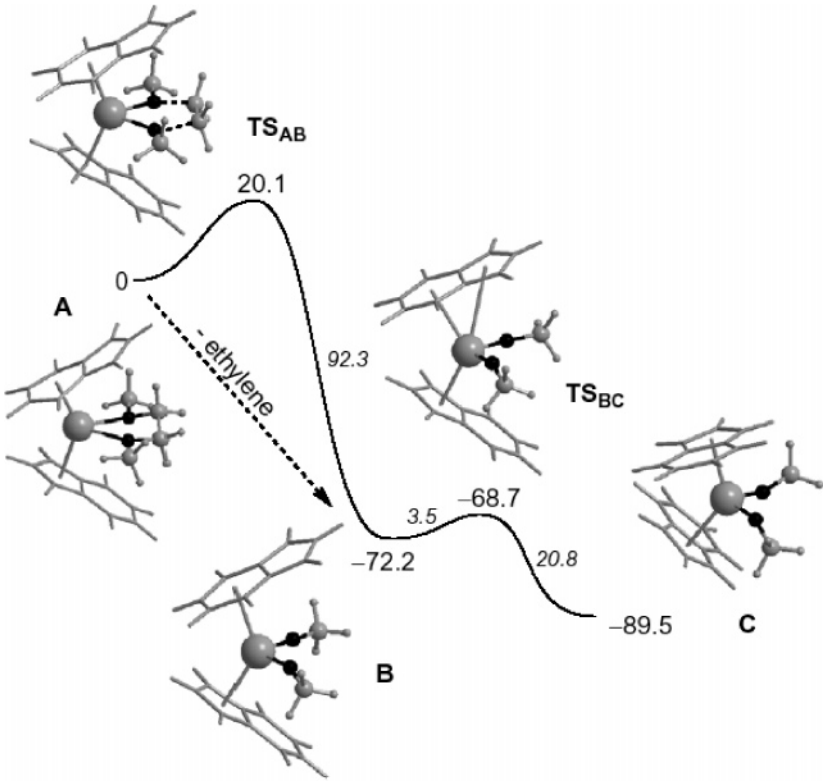

Figure 9. Free energy profile for the mechanism of C−O activation followed by indenyl haptotropic shift, starting from (η^6-C_9H_7)(η^5-C_9H_7)Zr(DME) (**A**). The minima and transition state were optimized (B3LYP/VDZP), and resulting structures are presented. The free energies (kcal/mol) are referenced to **A**, and the values in italics represent energy barriers. The O atoms are darkened.

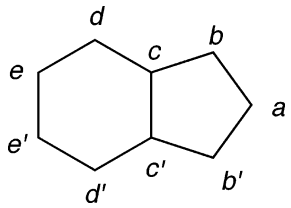

Figure 10. Labeling scheme for the indenyl ligand.

weakened (d = 2.90 and 3.30 Å, WI = 0.048 and 0.122). The first step, **A** → **B**, is the rate-limiting step with an accessible activation free energy of 20.1 kcal/mol, and the entire reaction is thermodynamically favorable, with $\Delta G = -89.5$ kcal/mol.

The first step to be taken to check the possibility of a mechanism where the indenyl haptotropic shift occurs before C−O bond cleavage is the calculation of the reaction path for C−O bond breaking in the (η^5-C_9H_7)$_2$Zr(DME) complex, **D**. In fact, should this process be less favorable than the equivalent reaction starting from the η^6,η^5 complex **A**, then the mechanisms on the left side of Figure 8 could be ruled out and the preferred pathway would be the one presented in Figure 9. The free energy profile for the reaction leading from (η^5-C_9H_7)$_2$Zr(DME) (**D**) to the final products, ethylene and the bis(methoxide) species, **C**, is depicted in Figure 11.

The profile presented in Figure 11 corresponds to a single-step pathway with simultaneous cleavage of the two C−O bonds in **D**, leading directly to the reaction products, being equivalent, in its general feature, to the first step of the path calculated for the reaction **A** → **C**, presented above. However, the reaction starting from (η^5-C_9H_7)$_2$Zr(DME) has a lower barrier, having an activation free energy of 10.9 kcal/mol,[16] about half of the value calculated when starting with **A**. The difference in activation energy between the two reactions can be traced to the structural characteristics of the corresponding transition states. **TS$_{DC}$** represents an even earlier transition state than **TS$_{AB}$**, as demonstrated by the shorter and stronger C−O bonds (d_{C-O} = 1.54 and 1.79 Å, WI = 0.469 and 0.724) and by a comparatively delayed formation of the C═C bond in the newly formed ethylene molecule (d_{C-O} = 1.47 Å, WI = 1.121). In other words, for the η^5,η^5 species, the structural changes that need to occur in the reactant (**D**) to reach the transition state (**TS$_{DC}$**) are less dramatic than the ones occurring in the

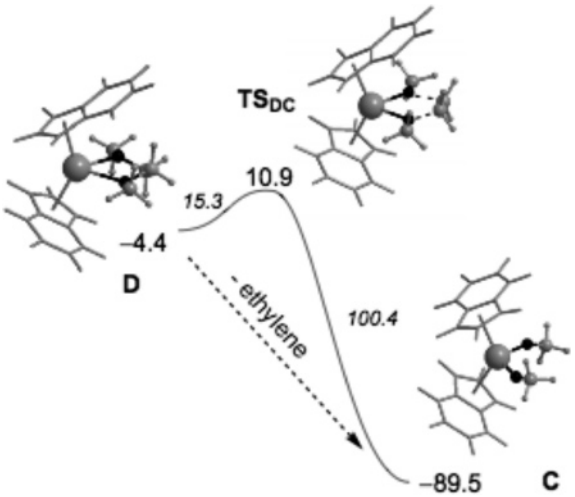

Figure 11. Free energy profile for the mechanism of C−O bond activation, starting from (η^5-C_9H_7)$_2$Zr(DME) (**D**). The minima and the transition state were optimized (B3LYP/VDZP), and the resulting structures are presented. The free energies (kcal/mol) are referenced to **A**, and the values in italics correspond to energy barriers. The O atoms are darkened.

(16) All free energies are referred to the initial reactant: [(η^6-C_9H_7)-(η^5-C_9H_7)Zr(DME)] (**A**).

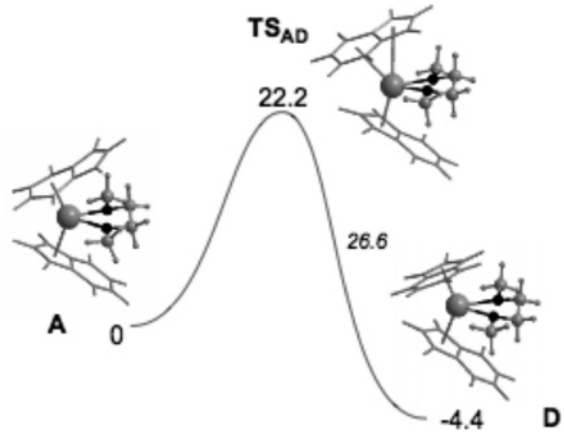

Figure 12. Free energy profile for the intramolecular haptotropic shift from η^6 to η^5 ring coordination in (η^6-C_9H_7)(η^5-C_9H_7)Zr(DME) (**A**). The minima and the transition state were optimized (B3LYP/VDZP), and the resulting structures are presented. The free energies (kcal/mol) are referenced to **A**, and the value in italics corresponds to the energy barrier. Oxygen atoms are darkened.

equivalent process with the compound of mixed hapticity (from **A** to $\mathbf{TS_{AB}}$), reflecting an easier reaction where the reactant has to move less along the reaction coordinate to attain the transition state. This is related to the stability differences of the minima involved in the two processes, especially the corresponding products (**B** is 17.3 kcal/mol less stable than **C**), and is a consequence of the zirconium−indenyl bonding in these complexes: **B** is an η^6,η^5 species, while **C** is an η^5,η^5 complex. Recent studies have demonstrated that metal to ligand back-donation is an important component of η^6-indenyl coordination.[3,17] Since both **B** and **C** are formally Zr(IV) complexes, there are no metal electrons available for back-donation, and thus, the bis η^5,η^5 hapticity found in typical Zr(IV) bent metallocene complexes is preferred.

Because C−O bond breaking and subsequent ethylene formation are more kinetically favorable from complex **D** than with **A**, mechanisms involving indenyl haptotropic shift before C−O cleavage (left side, Figure 8) were explored. In these cases, (η^5-C_9H_7)$_2$Zr(DME) corresponds to an intermediate in the overall reaction and its formation from the reactant, (η^6-C_9H_7)-(η^5-C_9H_7)Zr(DME), can be achieved by an intramolecular shift of the rings from η^6 to η^5 hapticity. The free energy profile for the haptotropic rearrangement is presented in Figure 12.

The preferred mechanism for intramolecular ring slippage from **A** to **D** occurs in a single-step transition state ($\mathbf{TS_{AD}}$) quite similar to the second step described above for the reaction **A** → **C** in what concerns Zr−indenyl coordination. The hapticity of the shifting indenyl ligand in $\mathbf{TS_{AD}}$ is between η^6 and η^5 coordination, and the relevant bond distances are equivalent to those in $\mathbf{TS_{BC}}$. The cleavage of the Zr−C bonds of the benzo portion is already achieved, as shown by the long and very weak interactions with $C_{e/e'}$ ($d_{Zr-Ce/e'}$ = 3.07 and 3.49 Å, WI = 0.023 and 0.133), and the formation of the new bonds between the metal and the carbon atoms of the five-membered ring is incipient, as demonstrated by a rather long Zr−C_a separation (3.72 Å), corresponding to a weak interaction (WI = 0.034). The coordination of DME to the zirconium atom is maintained throughout the entire process. Although the reaction is thermodynamically favored ($\Delta G = -4.4$ kcal/mol), the activation free energy for this step, **A** → **D**, is rather high (22.2 kcal/mol), being 2.1 kcal/mol higher than the overall activation energy obtained starting from the η^6,η^5 complex, **A** → **C** (Figure 9). The energetics of this step precludes such a step in the overall transformation associated with C−O bond cleavage.

A second route to the η^5,η^5 complex, **D**, is a dissociative mechanism involving initial loss of DME from **A**. In this pathway, loss of DME forms the sandwich complex, which then adds DME to yield **D**. The calculated free energy profile for this reaction is presented in Figure 13. Notably, a free energy difference of −4.4 kcal/mol, corresponding to an equilibrium constant of approximately 1700 M^{-1}, was computed, consistent with the experimental observation of a $K_{eq} > 200$ M^{-1}.[8] However, it should be noted that the computational studies involve unsubstituted indenyl ligands and the actual value for the free energy of DME coordination is likely to be attenuated by the sterically demanding ring substituents.

The profile calculated for the reaction **A** → **D** via a dissociative mechanism is comprised of six individual steps. The first two correspond to dissociation of DME from the η^6,η^5 adduct, **A**, and yield the sandwich complex (η^9-C_9H_7)(η^5-C_9H_7)-Zr, with an *anti* conformation of the two indenyl ligands (**F**). In the first of those steps, one of the two Zr−O bonds existing in **A** is broken, producing an adduct, **E**, similar to known bis-(indenyl)zirconium monoether compounds. The coordination mode of the indenyl ligand is maintained along the process **A** → **E**, and in the corresponding transition state, $\mathbf{TS_{AE}}$, the Zr−O bond is practically broken (d_{Zr-O} = 3.68 Å, WI = 0.033). The following step, **E** → **F**, corresponds to the cleavage of the second Zr−O bond with simultaneous rearrangement of one of the indenyl rings from η^6 to η^9 hapticity. As previously reported in the case of the THF adduct (η^6-C_9H_7)(η^5-C_9H_7)Zr(THF),[7] the reaction **E** → **F** clearly goes through a dissociative transition state ($\mathbf{TS_{EF}}$). Once $\mathbf{TS_{EF}}$ is reached, the Zr−O bond is practically broken (d_{Zr-O} = 3.22 Å, WI = 0.082) while the C_5 ring of the η^6 ring is not yet coordinated to Zr, as indicated by a very long (3.52 Å) and weak (WI = 0.094) Zr−C_a interaction.

The two steps in the middle of the profile in Figure 13 correspond to the indenyl slippage from η^9 to η^5 coordination in the sandwich complex. First there is reorientation of the indenyl ligands from an *anti* to a *gauche* conformation (**F** → **G**), then a shift of the η^9 to η^5 coordination (**G** → **H**), ending up with the bis η^5,η^5 sandwich complex, **H**. This process was thoroughly addressed before and will not be further discussed here.[3,7]

The final two steps in the **A** → **D** mechanism correspond to DME addition to **H**. Along this pathway there is consecutive formation of each new Zr−O bond, while the coordination mode of the two indenyl ligands remains unchanged. Coordination of the first DME oxygen atom goes through a transition state ($\mathbf{TS_{HI}}$) with a very long Zr−O interaction (4.24 Å), in what may be viewed as a van der Waals complex. In the last step of the profile presented in Figure 13, DME addition is completed by the formation of the second Zr−O bond, from the monodentate ether complex, **I**, yielding the bis η^5,η^5 DME species, **D**. In the transition state, $\mathbf{TS_{ID}}$, the new Zr−O bond is a long and weak interaction (d_{Zr}−O = 3.88 Å, WI = 0.029), but still significantly shorter than the one existing in $\mathbf{TS_{HI}}$.

The rate-limiting step in the reaction **A** → **D** corresponds to dissociation of DME from the (η^6-C_9H_7)(η^5-C_9H_7)Zr fragment, namely, the second step in the profile presented in Figure 13 (**E** → **F**), and is fully consistent with the observed kinetic isotope effect. The activation free energy associated with the reaction is quite accessible (15.2 kcal/mol) and is lower than the corresponding values for both C−O activation from the η^6,η^5 complex, **A**, and the intramolecular haptropic rearrangement.

(17) Veiros, L. F. *Organometallics* **2006**, *25*, 4698.

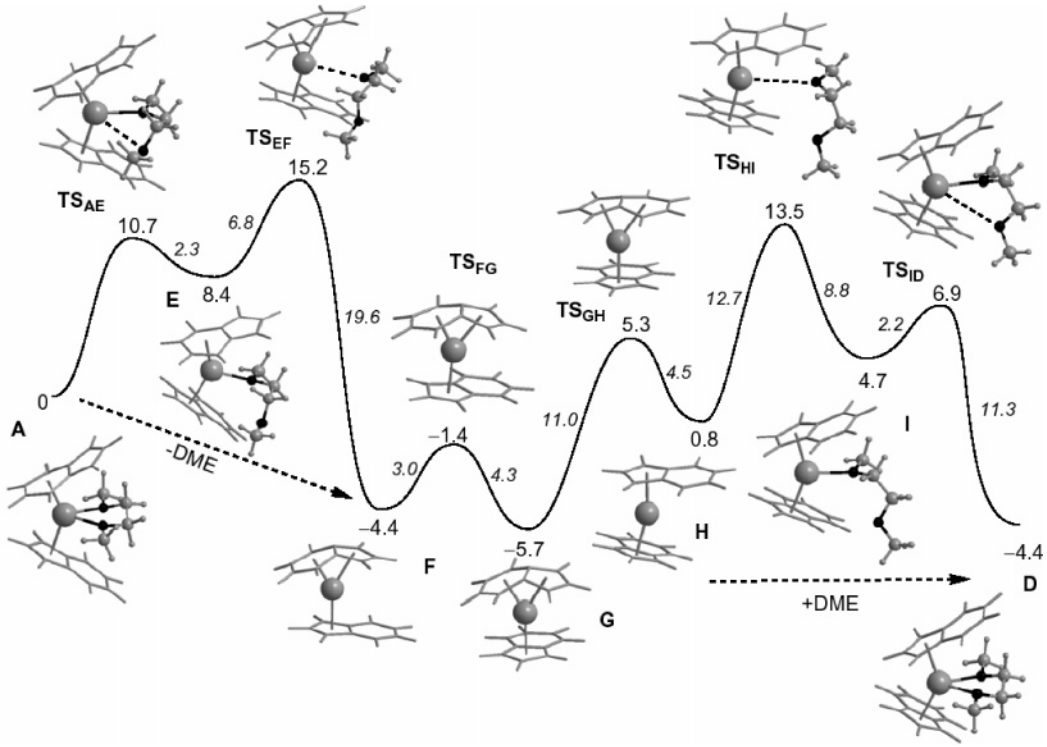

Figure 13. Free energy profile for the reaction (η^6-C_9H_7)(η^5-C_9H_7)Zr(DME) (**A**) to (η^5-C_9H_7)$_2$Zr(DME) (**D**) by a dissociative mechanism. The minima and the transition states were optimized (B3LYP/VDZP), and the resulting structures are presented. The free energies (kcal/mol) are referenced to **A**, and the values in parentheses represent energy barriers. The O atoms are darkened.

Thus, the most favorable mechanism calculated for the entire reaction, starting with (η^6-C_9H_7)(η^5-C_9H_7)Zr(DME) and ending with ethylene and the bis(indenyl)zirconium bis(methoxide) complex, (η^5-C_9H_7)$_2$Zr(OCH_3)$_2$, goes through a haptotropic rearrangement from an η^6 indenyl ring by means of a dissociative mechanism and then C−O bond breaking occurs in the resulting η^5,η^5 DME complex, (η^5-C_9H_7)$_2$Zr(DME), yielding the final products. This corresponds to the profile in Figure 13 followed by the one in Figure 11.

It is interesting to briefly compare the mechanism calculated here for C−O activation in the DME complexes and the one previously reported for the equivalent reactions with THF. The overall features of the two mechanisms are similar, as THF dissociation precedes C−H and C−O bond cleavage. However, in the THF case, the rate-limiting step is the final step of the reaction, that is, the bond activation step. For DME, it is the initial part of the mechanism that involves dissociation of the diether. This reflects the coordination characteristics of the two ethers, THF and DME. In fact, the chelate effect associated with DME coordination makes dissociation more difficult; the activation energy for ether dissociation starting from the η^6,η^5 adduct and ending up with the sandwich and free ether (**A** → **F**, Figure 13) is 15.2 kcal/mol in the case of DME and only 12.0 kcal/mol for the equivalent process with THF. On the other hand, the stability of the final products also makes a difference by facilitating the second part of the mechanism in the DME case. The activation energy is 10.9 kcal/mol for DME, corresponding to C−O bond breaking (**D** → **C**, Figure 9), while in the THF system it is 13.3 kcal/mol, corresponding to C−H activation. In fact for DME, two quite stable molecules are formed, ethylene and a Zr(IV) bent metallocene complex with two methoxide ligands. For THF cleavage, a single alkyl−alkoxide metallocycle is formed. The stability of the final products is reflected in the overall spontaneity of the reaction: $\Delta G = -89.5$ kcal/mol for DME and −54.4 kcal/mol for THF. It should be noted that these barriers are calculated for model compounds where steric effects and hence the true barriers may be attenuated.

Concluding Remarks

The combined experimental and computational studies reported in this work highlight the varied mechanistic pathways available for C−O and C−S bond cleavage by η^9,η^5 bis(indenyl)zirconium sandwich complexes. For aliphatic ethers and THF, C−H activation precedes C−O bond cleavage, while for DME, dissociation of the chelate is the rate-determining step. In contrast, the observed products from thioether cleavage are consistent with direct C−S addition, highlighting the weaker bond strength of the heavier chalcogen.

Experimental Section

General Considerations. All air- and moisture-sensitive manipulations were carried out using standard vacuum line, Schlenk, or cannula techniques or in an M. Braun inert atmosphere drybox containing an atmosphere of purified nitrogen. Solvents for air- and moisture-sensitive manipulations were initially dried and deoxygenated using literature procedures.[18] Benzene-d_6 and toluene-d_8 were distilled from sodium metal under an atmosphere of argon and stored over 4 Å molecular sieves or sodium metal. Solutions of 4.0 M HCl and 4.0 M DCl in dioxane were purchased from Aldrich and degassed before use. Ethylene-d_4 was purchased from Cambridge Isotope Laboratories and was used as received. **1**[1] and **1-DME**[8] were prepared according to literature procedures. Tetrahydrothiophene was purchased from Acros and dried over calcium hydride prior to use. Ethyl sulfide was purchased from Aldrich, while 3,6-dithiaoctane was purchased from Wako Pure Chemicals;

(18) Pangborn, A. B.; Giardello, M. A.; Grubbs, R. H.; Rosen, R. K.; Timmers, F. J. *Organometallics* **1996**, *15*, 1518.

both were dried over calcium hydride before use. All calibrated gas bulb experiments were conducted using a 31.6 mL bulb unless noted otherwise.

^{1}H and ^{13}C NMR spectra were recorded on a Varian Inova 400 spectrometer operating at 399.779 MHz (^{1}H) and 110.524 MHz (^{13}C). All chemical shifts are reported relative to $SiMe_4$ using ^{1}H (residual) or ^{13}C NMR chemical shifts of the solvent as a secondary standard. NOESY experiments were recorded on a Varian 500 Inova spectrometer operating at 499.920 MHz for ^{1}H and 125.704 MHz for ^{13}C. ^{2}H NMR spectra were recorded on a Varian Inova 500 spectrometer operating at 76.740 MHz, and the spectra were referenced using an internal benzene-d_6 standard.

Gradient-selected COSY spectra were acquired with a sweep width of 5.4 kHz. A total of 128 points were collected in the indirectly detected dimension with 4 scans and 2K points per increment. The resulting matrix was zero filled to 1K × 1K complex data points, and squared sinusoidal window functions were applied in both dimensions prior to Fourier transform. Gradient selected HSQC spectra were acquired with sweep widths of 5.6 and 21.4 kHz in ^{1}H and ^{13}C dimensions, respectively. A total of 200 complex points were collected in the indirectly detected dimension with 12 scans and 2K points per increment. The resulting matrix was zero filled to 1K × 1K complex data points, and Gaussian line-broadening window functions were applied in both dimensions prior to Fourier transform.

Mass spectrometry was performed on a Hewlett-Packard 5980A GC/MS equipped with a 5970 mass selective detector and a DB-1, 0.25 μm film, fused silica capillary column with an injection temperature of 35 °C, a ramp rate of 10 °C, and a final column temperature of 260 °C. Elemental analyses were performed at Robertson Microlit Laboratories, Inc., Madison, NJ.

Thermolysis of 1-DME and Characterization of (η^5-C_9H_5-1,3-$(SiMe_3)_2$)$_2$Zr$(OCH_3)_2$ (1-$(OMe)_2$). A J. Young NMR tube was charged with 0.015 g (0.021 mmol) of **1-DME** dissolved in approximately 0.5 mL of benzene-d_6. The resulting green solution was heated to 45 °C for 16 h. Monitoring the reaction by NMR spectroscopy revealed quantitative conversion and formation of an equimolar mixture of **1-(η^2-CH_2=CH_2)** and **1-$(OMe)_2$**. ^{1}H NMR (benzene-d_6): δ 0.30 (s, 36H, Si*Me*$_3$), 3.54 (s, 6H, OC*H*$_3$), 6.81 (s, 2H, Cp), 7.11 (m, 4H, Benzo), 7.72 (m, 4H, Benzo). ^{13}C NMR (benzene-d_6): δ 0.18 (Si*Me*$_3$), 59.33 (O*C*H$_3$), 113.96, 123.17, 124.74, 139.98, 140.85 (Cp/Benzo).

Thermolysis of 1-DEE and Characterization of (η^5-C_9H_5-1,3-$(SiMe_3)_2$)$_2$Zr$(O(CH_2)_2OEt)H$ (1-$(O(CH_2)_2OEt)H$). A J. Young NMR tube was charged with 0.018 g (0.030 mmol) of **1**, and approximately 0.5 mL of benzene-d_6 was added. By microsyringe, 42 μL (0.30 mmol) of diethoxyethane was then added to the tube. The resulting green solution was heated to 45 °C for 16 h. Monitoring the reaction by ^{1}H NMR spectroscopy established quantitative conversion and formation of an equimolar mixture of **1-(η^2-CH_2=CH_2)** and **1-$(O(CH_2)_2OEt)H$**. Removal of the solvent in vacuo followed by addition of benzene-d_6 allowed spectroscopic characterization of **1-$(O(CH_2)_2OEt)H$**. ^{1}H NMR (benzene-d_6): δ 0.48 (s, 18H, Si*Me*$_3$), 0.50 (s, 18H, Si*Me*$_3$), 1.11 (t, 8 Hz, 3H, C*H*$_3$), 3.00 (t, 5 Hz, 2H, OC*H*$_2$), 3.23 (q, 8 Hz, 2H, C*H*$_2$CH$_3$), 3.52 (t, 5 Hz, 2H, OC*H*$_2$), 5.24 (s, 2H, Cp), 5.28 (s, 1H, Zr-*H*), 6.74 (m, 2H, Benzo), 6.81 (m, 2H, Benzo) 7.32 (d, 7 Hz, 2H, Benzo), 7.53 (d, 7 Hz, 2H, Benzo). ^{13}C NMR (benzene-d_6): δ 1.83, 1.94 (Si*Me*$_3$), 15.49 (CH$_2$*C*H$_3$), 66.49, 70.64, 72.90 (O*C*H$_2$), 108.98, 117.49, 123.48, 124.16, 125.14, 125.62, 129.20, 133.87 (Cp/Benzo). One Cp/Benzo resonance not located.

Preparation of (η^5-C_9H_5-1,3-$(SiMe_3)_2$)$_2$Zr$(SCH_2CH_3)(CH_2CH_3)$ (1(SEt)Et). A J. Young NMR tube was charged with 0.085 g (0.139 mmol) of **1**. On the vacuum line, 245 Torr (0.42 mmol) of Et_2S was added to the tube at −196 °C. The tube was thawed, shaken, and allowed to stand overnight. The solvent was then removed in vacuo and the tube transferred into the drybox, where the residue was extracted with pentane, yielding 0.080 g (82%) of a red oil identified as **1-(SEt)Et**. ^{1}H NMR (benzene-d_6): δ 0.39 (s, 18H, Si*Me*$_3$), 0.40 (s, 18H, Si*Me*$_3$), 0.64 (q, 7 Hz, 2H, C*H*$_2$-CH$_3$), 1.18 (t, 7 Hz, 3H, CH$_2$C*H*$_3$), 1.36 (t, 7 Hz, 3H, CH$_2$C*H*$_3$), 2.59 (q, 7 Hz, 2H, SC*H*$_2$CH$_3$), 6.14 (s, 2H, Cp), 6.98−7.08 (br m, 4H, Benzo), 7.59 (d, 8 Hz, 2H, Benzo), 7.71 (d, 8 Hz, 2H, Benzo). ^{13}C NMR (benzene-d_6): δ 1.80, 1.92 (Si*Me*$_3$), 19.67, 21.35, 32.28 (CH$_2$CH$_3$), 58.31 (S*C*H$_2$CH$_3$), 117.39, 117.50, 124.42, 124.71, 127.09, 127.63, 132.98, 135.61, 137.02 (Cp/Benzo). Isolation of **1-(SEt)Et** as an oil precluded obtaining satisfactory combustion analysis.

Preparation of (η^5-C_9H_5-1,3-$(SiMe_3)_2$)$_2$Zr(*cyclo*-$SCH_2CH_2CH_2CH_2$) (1-*c*-$S(CH_2)_4$). This molecule was prepared in an identical procedure to **1-(SEt)Et** with 0.111 g (0.182 mmol) of **1** and 339 Torr (0.58 mmol) of THT from a 100.1 mL calibrated gas bulb. Recrystallization from pentane afforded 0.058 g (46%) of a red solid identified as **1-*c*-$S(CH_2)_4$**. Anal. Calcd for $C_{34}H_{54}Si_4SZr$: C, 58.48; H, 7.78. Found: C, 58.73; H, 7.42. ^{1}H NMR (benzene-d_6): δ 0.36 (s, 18H, Si*Me*$_3$), 0.40 (s, 18H, Si*Me*$_3$), 0.85 (dd, 4 Hz 2H, $SCH_2CH_2CH_2CH_2$), 1.14 (t, 4 Hz, 2H, $SCH_2CH_2CH_2CH_2$), 1.97 (m, 2H, $SCH_2CH_2CH_2CH_2$), 2.89 (t, 5 Hz, 2H, S*C*H$_2$CH$_2$CH$_2$CH$_2$), 6.00 (s, 2H, Cp), 7.02 (m, 4H, Benzo), 7.52 (d, 8 Hz, 2H, Benzo), 7.78 (d, 8 Hz, 2H, Benzo). ^{13}C NMR (benzene-d_6): δ 1.69, 1.82 (Si*Me*$_3$), 31.62 ($SCH_2CH_2CH_2CH_2$), 33.33 ($SCH_2CH_2CH_2CH_2$), 37.19 ($SCH_2CH_2CH_2CH_2$), 63.72 (S*C*H$_2$CH$_2$CH$_2$CH$_2$), 116.30, 119.67, 124.52, 124.69, 126.90, 131.93, 135.80, 136.92, 145.38 (Cp/Benzo).

Observation of (η^6-C_9H_5-1,3-$(SiMe_3)_2$)(η^5-C_9H_5-1,3-$(SiMe_3)_2$)-Zr$(EtSCH_2CH_2SEt)$ (1-DTO). A J. Young tube was charged with 0.012 g (0.020 mmol) of **1** and approximately 0.4 mL of toluene-d_8. To the burgundy solution was added 3 μL (0.020 mmol) of 3,6-dithiaoctane, and the tube was immediately immersed in an acetone/dry ice bath. Within 5 min, the sample was placed in the NMR probe precooled to −45 °C, and **1-DTO** was monitored. The adduct is stable for a few hours at −45 °C, over which time **1-DTO** converts to **1-$(SEt)_2$**. ^{1}H NMR (toluene-d_8, −45 °C): δ 0.29 (s, 18H, Si*Me*$_3$), 0.54 (s, 18H, Si*Me*$_3$), 1.06 (br s, 6H, SCH$_2$C*H*$_3$), 1.81 (br, 4H, SC*H*$_2$), 2.30 (br, 4H, SC*H*$_2$), 4.29 (br s, 2H, Benzo), 4.65 (s, 1H, Cp), 6.61 (br, 2H, Benzo), 6.71 (br, 2H, Benzo), 6.96 (s, 1H, Cp), 7.20 (br, 2H, Benzo). ^{13}C NMR (toluene-d_8, −45 °C): δ 1.98, 2.95 (Si*Me*$_3$), 14.70 (SCH$_2$*C*H$_3$), 23.97 (S*C*H$_2$), 32.80 (S*C*H$_2$-CH$_3$), 118.22, 140.31 (Cp), 82,68, 101.90, (Benzo), 112.05, 121.90, 122.55, 126.20, 134.00 (Cp/Benzo). One Cp/Benzo resonance not located.

Preparation of (η^5-C_9H_5-1,3-$(SiMe_3)_2$)$_2$Zr$(SCH_2CH_3)_2$ (1-$(SEt)_2$). A J. Young NMR tube was charged with 0.025 g (0.041 mmol) of **1**. Using a microliter syringe, 6 μL (0.040 mmol) of 3,6-dithiaoctane was added to the tube. The tube was shaken, and the reaction was complete in less than 5 min, giving a light orange solution. The solvent was then removed in vacuo and the tube transferred into the drybox, where the residue was recrystallized in pentane, yielding 0.016 g (53%) of an orange solid identified as **1-$(SEt)_2$**. Anal. Calcd for $C_{34}H_{56}Si_4S_2Zr$: C, 55.75; H, 7.71. Found: C, 55.51; H, 7.63. ^{1}H NMR (benzene-d_6): δ 0.43 (s, 36H, Si*Me*$_3$), 1.24 (t, 8 Hz, 3H, SCH$_2$C*H*$_3$), 2.86 (q, 8 Hz, 2H, SC*H*$_2$CH$_3$), 6.02 (s, 2H, Cp), 6.97(m, 4H, Benzo), 7.55 (m, 4H, Benzo). ^{13}C NMR (benzene-d_6): δ 1.75 (Si*Me*$_3$), 20.14 (SCH$_2$*C*H$_3$), 38.40 (S*C*H$_2$CH$_3$), 119.31, 124.96, 126.78, 131.95, 136.26 (Cp/Benzo).

General Procedure for Kinetic Isotope Effect Determinations. A flame-dried J. Young NMR tube was charged with 300 μL of a benzene-d_6 stock solution containing 0.025 M **1-DME** and 0.025 M **1-DME-d_{10}** and 200 μL of a 0.02 M benzene-d_6 solution containing sublimed ferrocene. The tube was quickly shaken and its contents were frozen in liquid nitrogen. The tube was then transferred to a preheated NMR probe at 45 °C, and the disappearance of starting material and subsequent appearance of product

(**1-(OMe)$_2$** and **1-(OMe-d_3)$_2$**) were measured by an arrayed ^{1}H NMR experiment. Typically the time interval between data collection was 30 min. Spectra were integrated versus the ferrocene standard for four runs at times of 1, 4, 8, and 12 h. A negligible kinetic isotope effect was observed at all times.

Computational Details. All calculations were performed using the Gaussian 98 software package[19] and the B3LYP hybrid functional, without symmetry constraints on models with unsubstituted indenyl ligands. That functional includes a mixture of Hartree−Fock[20] exchange with DFT[14] exchange−correlation, given by Becke's three-parameter functional[21] with the Lee, Yang, and Parr correlation functional, which includes both local and nonlocal terms.[22,23] The LanL2DZ basis set[24] augmented with an f-polarization function[25] was used for Zr, and a standard 6-31G(d,p)[26] for the remaining elements. Transition-state optimizations were performed with the synchronous transit-guided quasi-Newton method (STQN) developed by Schlegel et al.[27] Frequency calculations were performed to confirm the nature of the stationary points, yielding one imaginary frequency for the transition states and none for the minima. Each transition state was further confirmed by following its vibrational mode downhill on both sides and obtaining the minima presented on the energy profiles. Free energies were obtained at 298.15 K and 1 atm by conversion of the zero-point-corrected electronic energies with the thermal energy corrections based on the calculated structural and vibrational frequency data. The Wiberg indices[15] used in the text to evaluate bond strength resulted from a natural population analysis (NPA).[28]

Acknowledgment. We thank the National Science Foundation (CAREER Award to P.J.C. and pre-doctoral fellowship to C.A.B.) for financial support. P.J.C. also acknowledges the Research Corporation for a Cottrell Scholarship and the Packard Foundation for a fellowship in science and engineering. We also thank Mr. Thomas McCarrick for assistance with acquisition of gas-phase infrared spectra.

Supporting Information Available: All atomic coordinates for DFT-optimized species. Experimental details for the synthesis and cleavage of *cis*-1,2-DME along with gas-phase infrared spectra following C−O bond cleavage.

OM0701120

(19) Frisch, M. J.; Trucks, G. W.; Schlegel, H. B.; Scuseria, G. E.; Robb, M. A.; Cheeseman, J. R.; Zakrzewski, V. G.; Montgomery, J. A., Jr.; Stratmann, R. E.; Burant, J. C.; Dapprich, S.; Millam, J. M.; Daniels, A. D.; Kudin, K. N.; Strain, M. C.; Farkas, O.; Tomasi, J.; Barone, V.; Cossi, M.; Cammi, R.; Mennucci, B.; Pomelli, C.; Adamo, C.; Clifford, S.; Ochterski, J.; Petersson, G. A.; Ayala, P. Y.; Cui, Q.; Morokuma, K.; Malick, D. K.; Rabuck, A. D.; Raghavachari, K.; Foresman, J. B.; Cioslowski, J.; Ortiz, J. V.; Stefanov, B. B.; Liu, G.; Liashenko, A.; Piskorz, P.; Komaromi, I.; Gomperts, R.; Martin, R. L.; Fox, D. J.; Keith, T.; Al-Laham, M. A.; Peng, C. Y.; Nanayakkara, A.; Gonzalez, C.; Challacombe, M.; Gill, P. M. W.; Johnson, B. G.; Chen, W.; Wong, M. W.; Andres, J. L.; Head-Gordon, M.; Replogle, E. S.; Pople, J. A. *Gaussian 98*, revision A.7; Gaussian, Inc.: Pittsburgh, PA, 1998.

(20) Hehre, W. J.; Radom, L.; Schleyer, P. v. R.; Pople, J. A. *Ab Initio Molecular Orbital Theory*; John Wiley & Sons: New York, 1986.

(21) Becke, A. D. *J. Chem. Phys.* **1993**, *98*, 5648.

(22) Miehlich, B.; Savin, A.; Stoll, H.; Preuss, H. *Chem. Phys. Lett.* **1989**, *157*, 200.

(23) Lee, C.; Yang, W.; Parr, G. *Phys. Rev. B* **1988**, *37*, 785.

(24) (a) Dunning, T. H., Jr.; Hay, P. J. *Modern Theoretical Chemistry*; Schaefer, H. F., III, Ed.; Plenum: New York, 1976; Vol. 3, p 1. (b) Hay, P. J.; Wadt, W. R. *J. Chem. Phys.* **1985**, *82*, 270. (c) Wadt, W. R.; Hay, P. J. *J. Chem. Phys.* **1985**, *82*, 284. (d) Hay, P. J.; Wadt, W. R. *J. Chem. Phys.* **1985**, *82*, 2299.

(25) Ehlers, A. W.; Böhme, M.; Dapprich, S.; Gobbi, A.; Höllwarth, A.; Jonas, V.; Köhler, K. F.; Stegmann, R.; Veldkamp, A.; Frenking, G. *Chem. Phys. Lett.* **1993**, *208*, 111.

(26) (a) Ditchfield, R.; Hehre, W. J.; Pople, J. A. *J. Chem. Phys.* **1971**, *54*, 724. (b) Hehre, W. J.; Ditchfield, R.; Pople, J. A. *J. Chem. Phys.* **1972**, *56*, 2257. (c) Hariharan, P. C.; Pople, J. A. *Mol. Phys.* **1974**, *27*, 209. (d) Gordon, M. S. *Chem. Phys. Lett.* **1980**, *76*, 163. (e) Hariharan, P. C.; Pople, J. A. *Theor. Chim. Acta* **1973**, *28*, 213.

(27) (a) Peng, C.; Ayala, P. Y.; Schlegel, H. B.; Frisch, M. J. *J. Comput. Chem.* **1996**, *17*, 49. (b) Peng, C.; Schlegel, H. B. *Isr. J. Chem.* **1994**, *33*, 449.

(28) (a) Carpenter, J. E.; Weinhold, F. *J. Mol. Struct. (THEOCHEM)* **1988**, *169*, 41. (b) Carpenter, J. E. Ph.D. thesis, University of Wisconsin (Madison WI), 1987. (c) Foster, J. P.; Weinhold, F. *J. Am. Chem. Soc.* **1980**, *102*, 7211. (d) Reed, A. E.; Weinhold, F. *J. Chem. Phys.* **1983**, *78*, 4066. (e) Reed, A. E.; Weinhold, F. *J. Chem. Phys.* **1983**, *78*, 1736. (f) Reed, A. E.; Weinstock, R. B.; Weinhold, F. *J. Chem. Phys.* **1985**, *83*, 735. (g) Reed, A. E.; Curtiss, L. A.; Weinhold, F. *Chem. Rev.* **1988**, *88*, 899. (h) Weinhold, F.; Carpenter, J. E. *The Structure of Small Molecules and Ions*; Plenum: New York, 1988; p 227.